

## Effects of Steel Fibers on Properties of Concrete for Energy Storage Application

A.A. Adeyanju and K. Manohar

Department of Mechanical and Manufacturing Engineering,  
University of the West Indies, St. Augustine, Trinidad, West Indies

---

**Abstract:** An experimental study on the thermal and mechanical properties of steel-fiber-reinforced concrete for solar/thermal energy storage purposes is presented in this report. It takes into account the results of measurements of thermal conductivity, thermal resistivity, thermal diffusivity and the results of compressive strength as well as thermal energy storage calculated from the knowledge of the above measured parameters. The Experimental testing method is described as well based upon the linear heat source theory, it requires the use of a special probe to be inserted into the sample. The experimental programme was forwarded to test concrete aggregate mixtures with three different sizes of steel fibers and one plain concrete. The measurements were carried out from the pouring time of cubic samples and were ended up when hardened conditions were achieved. The results indicate that the steel fibers have influence on the thermal properties of the concretes tested.

**Key words:** Steel, fiber, reinforced, concrete, thermal, properties, energy, storage

---

### INTRODUCTION

The electrical output of a solar thermal electric plant is inherently in a state of change, being dictated by both predictable and unpredictable variations (the influences of time and weather). In either event, utility system needs may require a fully functional storage system to mitigate the changes in solar radiation or to meet demand peaks. A distinct advantage of solar thermal power plants compared with other renewable energies such as Photovoltaics (PV) and wind is the possibility of using relatively cheap storage systems. That is storing the thermal energy itself. Storing electricity is much more expensive.

Thermal Energy Storage (TES) option can collect energy in order to shift its delivery to a later time or to smooth out the plant output during intermittently cloudy weather conditions (Adeyanju and Manohar, 2009). Hence, the operation of a solar thermal power plant can be extended beyond periods of no solar radiation without the need to burn fossil fuel. Times of mismatch between energy supply by the sun and energy demand can be reduced.

When used with integrated solar combined cycle systems, energy storage could provide another important advantage. If the plant operates at base load, it will operate at full load only when enough solar energy is available. At part load, the turbine efficiency can decrease

considerably. If fossil energy is used to augment turbine load (through the use of duct firing, a heat transfer fluid heater or a backup boiler) when solar is not available, the plant converts that fossil fuel at a substantially lower efficiency than if it had been used directly in the combined cycle. Using thermal energy storage instead of a fossil burner can help to overcome this problem.

Economic thermal storage is a key technological issue for the future success of solar thermal technologies. The purpose of this study is to investigate experimentally, the effects of the addition of steel fibers to thermal properties of concrete.

Besides high thermal durability, the storage concrete has to fulfill numerous requirements. For example, a high heat capacity and thermal conductivity will reduce the costs of the heat exchanger and thermal insulation.

Research on closely-spaced wires and random metallic fibers in the late 1950's and early 1960's was the basis for a patent on Steel Fiber Reinforced Concrete (SFRC) based on fiber spacing. The Portland Cement Association (PCA) investigated fiber reinforcement in the late 1950's. Principles of composite materials were applied to analyze fiber reinforced concrete. The addition of fibers was shown to increase toughness much more than the first crack strength in these tests. Another patent based on bond and the aspect ratio of the fibers was granted in 1972. Since, the time of these original fibers many new steel fibers have been produced.

Steel fiber reinforced concrete is concrete made of hydraulic cements containing fine or fine and coarse aggregate and discontinuous discrete steel fibers. In tension, SFRC fails only after the steel fiber breaks or is pulled out of the cement matrix.

Properties of SFRC in both the freshly mixed and hardened state including durability are a consequence of its composite nature. The mechanics of how the fiber reinforcement strengthens concrete or mortar, extending from the elastic pre-crack state to the partially plastic post-cracked state is a continuing research topic. One approach to the mechanics of SFRC is to consider it a composite material whose properties can be related to the fiber properties (volume percentage, strength, elastic modulus and a fiber bonding parameter of the fibers), the concrete properties (strength, volume percentage and elastic modulus) and the properties of the interface between the fiber and the matrix. A more general and current approach to the mechanics of fiber reinforcing assumes a crack arrest mechanism based on fracture mechanics. In this model, the energy to extend a crack and de-bond the fibers in the matrix relates to the properties of the composite.

**Types of fiber:** Steel fibers intended for reinforcing concrete are defined as short, discrete lengths of steel having an aspect ratio (ratio of length to diameter) from about 20-100 with any of several cross-sections and that are sufficiently small to be randomly dispersed in an unhardened concrete mixture using usual mixing procedures.

ASTM provides a classification for four general types of steel fibers based upon the product used in their manufacture (ASTM C1018-89, 1991):

- **Type I:** Cold-drawn wire
- **Type II:** Cut sheet
- **Type III:** Melt-extracted
- **Type IV:** Other fibers

The Japanese Society of Civil Engineers (JSCE) has classified steel fibers based on the shape of their cross-section (JCI, 1983):

- **Type 1:** Square section
- **Type 2:** Circular section
- **Type 3:** Crescent section

The composition of steel fibers generally includes carbon steel (or low carbon steel, sometimes with alloying constituents) or stainless steel. Different applications may require different fiber compositions.

**Fiber properties:** The fiber strength, stiffness and the ability of the fibers to bond with the concrete are important fiber reinforcement properties. Bond is dependent on the aspect ratio of the fiber. Typical aspect ratios range from about 20-100 while length dimensions range from 6.4-76 mm.

Steel fibers have a relatively high strength and modulus of elasticity, they are protected from corrosion by the alkaline environment of the cementitious matrix and their bond to the matrix can be enhanced by mechanical anchorage or surface roughness. Long term loading does not adversely influence the mechanical properties of steel fibers. In particular environments such as high temperature refractory applications, the use of stainless steel fibers may be required. Various grades of stainless steel, available in fiber form, respond somewhat differently to exposure to elevated temperature and potentially corrosive environments. The user should consider all these factors when designing with steel fiber reinforced refractory for specific applications.

American Society for Testing and Materials (ASTM) establishes minimum tensile strength and bending requirements for steel fibers as well as tolerances for length, diameter (or equivalent diameter) and aspect ratio. The minimum tensile yield strength required by ASTM is 345 MPa while the Japanese Society of Civil Engineers (JSCE) specification requirement is 552 MPa.

**Manufacturing methods for steel fibers:** Round, straight steel fibers are produced by cutting or chopping wire, typically wire having a diameter between 0.25-1.00 mm. Flat, straight steel fibers having typical cross sections ranging from 0.15-0.64 mm thickness by 0.25-2.03 mm width are produced by shearing sheet or flattening wire (Fig. 1). Crimped and deformed steel fibers have been produced with both full-length crimping or bent or enlarged at the ends only. Some fibers have been deformed by bending or flattening to increase mechanical bonding. Some fibers have been collated into bundles to facilitate handling and mixing. During mixing, the bundles separate into individual fibers (ACI Committee, 1982).

Fibers are also produced from cold drawn wire that has been shaved down in order to make steel wool. The remaining wires have a circular segment cross-section and may be crimped to produce deformed fibers. Also available are steel fibers made by a machining process that produces elongated chips. These fibers have a rough, irregular surface and a crescent-shaped cross section.

Steel fibers are also produced by the melt-extraction process. This method uses a rotating wheel that contacts a molten metal surface, lifts off liquid metal and rapidly solidifies it into fibers. These fibers have an irregular surface and crescent shaped cross-section.



Fig. 1: Cubic shaped concrete samples

**Properties of freshly-mixed SFRC:** The properties of SFRC in its freshly mixed state are influenced by the aspect ratio of the fiber, fiber geometry, its volume fraction, the matrix proportions and the fiber-matrix interfacial bond characteristics. For conventionally placed SFRC applications, adequate workability should be insured to allow placement, consolidation and finishing with a minimum of effort while providing uniform fiber distribution and minimum segregation and bleeding. For a given mixture, the degree of consolidation influences the strength and other hardened material properties as it does for plain concrete.

In the typical ranges of volume fractions used for cast-in-place SFRC (0.25-1.5 volume percent), the addition of steel fibers may reduce the measured slump of the composite as compared to a non-fibrous mixture in the range of 25-100 mm. Since, compaction by mechanical vibration is recommended in most SFRC applications, assessing the workability of a SFRC mixture with either the Vebe consist-meter as described in the British Standards Institution Standard or by ASTM Inverted Slump-cone. Time is recommended rather than the conventional slump measurement. A typical relationship between slump, Vebe time and Inverted Slump-cone time is available. Studies have established that a mixture with a relatively low slump can have good consolidation properties under vibration (ASTM C1018-89, 1991). Slump loss characteristics with time for SFRC and non-fibrous concrete are similar. In addition to the above considerations, the balling of fibers must be avoided.

A collection of long thin steel fibers with an aspect ratio  $>100$  if shaken together will tend to interlock to form a mat or ball which is very difficult to separate by vibration alone. On the other hand, short fibers with an aspect ratio,  $<50$  are not able to interlock and can easily be dispersed by vibration. However as shown under hardened concrete, a high aspect ratio is desired for many improved mechanical properties in the hardened state.

The tendency of a SFRC mixture to produce balling of fibers in the freshly mixed state has been found to be a function of the maximum size and the overall gradation of the aggregate used in the mixture, the aspect ratio of the fibers, the volume fraction, the fiber shape and the method of introducing the fibers into the mixture.

The larger the maximum size aggregate and aspect ratio, the less volume fraction of fibers can be added without the tendency to ball. Guidance for determining the fiber sizes and volumes to achieve adequate hardened composite properties and how to balance these needs against the mix proportions for satisfactory freshly mixed properties is discussed later.

**Preparation technologies:** Mixing of SFRC can be accomplished by several methods with the choice of method depending on the job requirements and the facilities available. It is important to have a uniform dispersion of the fibers and to prevent the segregation or balling of the fibers during mixing.

Balling of the fibers during mixing is related to a number of factors. The most important factors appear to be the aspect ratio of the fibers, the volume percentage of fibers, the maximum size and gradation of the aggregates and the method of adding the fibers to the mixture. As the 1st 3 of these factors increase the tendency for balling increases.

**Mix proportions:** Compared to conventional concrete, some SFRC mixtures are characterized by higher cement content, higher fine aggregate content and decreasing slump with increasing fiber content. Since consolidation with mechanical vibration is recommended in most SFRC applications, assessing the workability of a SFRC mixture Inverted Slump-cone time or the Vebe test is recommended rather than the conventional slump measurement.

Conventional admixtures and pozzolans are commonly used in SFRC mixtures for air entrainment, water reduction, workability and shrinkage control. Test results indicate that lightweight SFRC can be formulated with minor modifications. Also, experience has shown that if the combined fine and coarse aggregate gradation envelopes as shown in the Table 1 are met, the tendency to form fiber balls is minimized and workability is enhanced (Balaguru and Shah, 1992).

**Mixing methods:** It is very important that the fibers be dispersed uniformly throughout the mixture. This must be done during the batching and mixing phase. Several mixing sequences have been successfully used including the following:

Table 1: Range of proportions for normal weight steel fiber reinforced concrete

Mix parameters	Maximum aggregate size		
	8 mm	18 mm	36 mm
Cement (kg m <sup>-3</sup> )	355-595	295-535	280-415
w/c ratio	0.35-0.45	0.35-0.50	0.35-0.55
Fine/coarse aggregate ratio	45-60	45-55	40-55
Entrained air (%)	4-8	4-6	4-5
Deformed fiber	0.4-1.0	0.3-0.8	0.2-0.7
Smooth fiber	0.8-2.0	0.6-1.6	0.4-1.4

ACI Committee (1982)

Add the fibers to the truck mixer after all other ingredients including the water have been added and mixed. Steel fibers should be added to the mixer hopper at the rate of about 45 kg min<sup>-1</sup> with the mixer rotating at full speed. The fibers should be added in a clump-free state so that the mixer blades can carry the fibers into the mixer. The mixer should then be slowed to the recommended mixing speed and mixed for 40-50 revolutions. Steel fibers have been added manually by emptying the containers into the truck hopper or via a conveyor belt or blower. The steel fibers can be added using the following method (Balaguru and Shah, 1992):

- Add the fibers to the aggregate stream in the batch plant before the aggregate is added to the mixer. Steel fibers can be added manually on top of the aggregates on the charging conveyor belt or via another conveyor emptying onto the charging belt. The fibers should be spread out along the conveyor belt to prevent clumping
- Add the fibers on top of the aggregates after they are weighed in the batcher. The normal flow of the aggregates out of the weigh batcher will distribute the fibers throughout the aggregates. Steel fibers can be added manually or via a conveyor

SFRC delivered to projects should conform to the applicable provisions. For currently used manual steel fiber charging methods, workers should be equipped with protective gloves and goggles. It is essential that tightly bound fiber clumps be broken up or prevented from entering the mix. It is recommended that the method of introducing the steel fibers into the mixture be proven in the field during a trial mix.

**Theory:** Thermal properties analyzer calculates its values for thermal conductivity, resistivity and diffusivity by monitoring the dissipation of heat from a line heat source given a known voltage. The equation for radial heat conduction in a homogeneous, isotropic medium is given by:

$$\frac{\partial T}{\partial t} = \alpha \left\{ \frac{\partial^2 T}{\partial r^2} + r^{-1} \frac{\partial T}{\partial r} \right\} \quad (1)$$

Where:

T = Temperature (°C)

t = Time (sec)

α = The thermal diffusivity (m<sup>2</sup> sec<sup>-1</sup>)

r = Radial distance (m)

When a long, electrically heated probe is introduced into a medium, the rise in temperature from initial temperature, at some distance from the probe is:

$$T - T_0 = \left( \frac{q}{4\pi K_h} \right) \text{Ei} \left( \frac{-r^2}{4\alpha t} \right) \quad (2)$$

Where:

q = The heat produced per unit length per unit time (W/m)

K<sub>h</sub> = The thermal conductivity of the medium (W/m°C)

E<sub>i</sub> = The exponential integral function

$$-\text{Ei}(-a) = \int_a^\infty \frac{1}{u} \exp(-u) du = -\gamma - \ln \left( \frac{r^2}{4\alpha t} \right) + \frac{r^2}{4\alpha t} - \left( \frac{r^2}{8\alpha t} \right) + \dots \quad (3)$$

With a = r<sup>2</sup>/4αt and γ is Euler's constant (0.5772) when t is large, the higher order terms can be ignored so combining Eq. 2 and 3 yields:

$$T - T_0 \cong \frac{q}{4\pi K_h} \left( \ln(t) - \gamma - \ln \left( \frac{-r^2}{4\alpha} \right) \right) \quad (4)$$

It is apparent from the relationship between thermal conductivity ΔT = T-T<sub>0</sub> and shown in Eq. 4 that ΔT and ln(t) are linearly related with a slope m = q/4πK<sub>h</sub>. Linearly regressing ΔT on ln(t) yields a slope that after rearranging gives the thermal conductivity as:

$$K_h = \frac{q}{4\pi m} \quad (5)$$

Where, q is known from the power supplied to the heater. The diffusivity can also be obtained from Eq. 4. The intersection of the regression line with the t-axis (ΔT = 0) gives:

$$\ln(t_0) = \left( \gamma + \ln \left( \frac{-r^2}{4\alpha} \right) \right) \quad (6)$$

From the calculated t<sub>0</sub> {from the intercept of ΔT vs. ln(t) and finite r}, Eq. 6 gives the diffusivity.

## MATERIALS AND METHODS

**Composition and preparation of the concrete cube:** The experiments and the test specimens used were described in detail in earlier studies (Adeyanju *et al.*, 2010) and will

therefore be only briefly described in this study. The type of aggregate influences the thermal properties of concrete and hence limestone and quartzite were used in the concrete mix (Table 2). Further to compare the performance of fiber-reinforced concrete with that of plain concrete, three types of concrete samples (A-D) were investigated and the compositions were shown in Table 3. As reinforcement, corrugated steel fibers were used. The fibers had a length of 5 cm, an equivalent diameter of 0.09 cm and an aspect ratio of 57. The weight percentage of the steel fibers in the concrete was approximately  $0.02 \text{ kg m}^{-3}$ . The steel fibers were added to the fresh concrete and mixed for about 2 min to ensure uniform dispersion. In making the concrete test cube, Portland cement, quartzite (sharp sand) and gravel (limestone) provided by the University of West Indies concrete laboratory were used. After consideration of various mixtures of sand and gravel, the proportion of 55% sand to 45% gravel by weight was chosen though the proportioning was actually done by loose volumes. These proportions lie between the coarser mixtures that are frequently used and the mixtures that have larger percentages of sand which produced an easily worked mixture. The aggregate of this mixture had a weight of  $3 \text{ kg}/0.001 \text{ m}^3$  of concrete cube. One consistency was used in the concrete mixture which is referred to as 100% water content. This consistency was such that freshly moulded concrete in cubic form of size  $0.1 \times 0.1 \text{ m}$  was made. Table 2 shows the mix proportions of different constituents for the mixtures tested, together with concrete and steel data for the four batches. Vibrators were used to consolidate the concrete. The forms were removed from the mould after the concrete had set 24 h. The forms were then stored in damp sand for 14 days and later removed to a dry room. They were all thoroughly dry when tested. The appearance of the cubic shaped concrete is shown in Fig. 1. The measured thermal properties were the thermal conductivity, thermal resistivity and thermal diffusivity of the concretes samples. All measurements were made with commercially available instruments. Full details of the instruments and the test procedure are given in Adeyanju *et al.* (2010).

**Sample testing of concrete mixes:** Concrete tests are administered to samples to learn about their properties. The most common concrete tests carried out in this study are the Conductivity test, Diffusivity test, Slump test and the Compressive Strength test.

**The Slump test:** The Slump test measures the workability and consistency of a concrete sample. A slump cone (30.48 cm tall) or a mini slump cone (10.16 cm tall), a tamping rod (1.5875 cm diameter x 60.96 cm tall) and concrete mix is required to complete the Slump test. To complete the Slump test, the Slump-cone is filled with concrete mix that amounts to the height and rodded with the tamping rod 25 times. This process is repeated 3 times until the cone is full. Then the excess cement is removed using the tamping rod. Immediately after the cement is removed, the slump cone is slowly lifted above the concrete mix which should be in the shape of a cone. Within 2.5 min, the difference between the concrete mix height and the slump cone height should be measured.

This value is known as the slump value. While individually slump values do not relay a large amount of information, a set of slump values show the consistency of the workability of the concrete mix; all the slump values should have approximately the same slump in order to have consistent workability. The slump value for the samples tested in this study is zero.

**The Compressive Strength test:** The Compressive Strength test measures the compressive force a concrete sample is able to withstand. A concrete sample (cube), a compressive test machine and safety glasses are required to complete this test. The seven concrete cube samples used for this test are all having dimension of  $0.1 \times 0.1 \text{ m}$ . After the sample is cured, it is placed between two metal plates in the compressive test machine shown in Fig. 2. The machine applies force increasing at a constant rate upon the sample. When the sample fails, the load applied is recorded in Table 3; this value is known as the

Table 2: Composition of concrete mixtures used for test

Properties	Samples			
	A	B	C	D
Water content (L)	0.28	0.28	0.28	0.28
Cement content ( $\text{kg m}^{-3}$ )	0.90	0.90	0.90	0.90
<b>Aggregate:</b>				
Quartzite ( $\text{kg m}^{-3}$ )	1.10	1.10	1.10	1.10
Limestone ( $\text{kg m}^{-3}$ )	1.00	1.00	1.00	1.00
Aggregate/cement	2.33	2.33	2.33	2.33
Water/cement	0.31	0.31	0.31	0.31
Steel fibers quantity ( $\text{kg m}^{-3}$ )	-	0.02	0.02	0.02
Steel fibers length (cm)	-	5.00	2.50	1.00
Steel fibers length equivalent diameter (cm)		0.09	0.09	0.09
Steel fibers/aggregate (%)	-	0.66	0.66	0.66

Table 3: Compressive strength of concrete specimens

Samples	Cast date	Date tested	Age (days)	Specimen size and type (mm)	Weight (kg)	Density ( $\text{kg m}^{-3}$ )	Compressive strength (KN)	Failure load ( $\text{N mm}^{-2}$ )
A	10/3/11	7/4/11	28	100 (cube)	2.55	2550	556	55.6
B	10/3/11	7/4/11	28	100 (cube)	2.87	2870	669	66.9
C	10/3/11	7/4/11	28	100 (cube)	2.85	2850	650	65.0
D	10/3/11	7/4/11	28	100 (cube)	2.83	2490	654	65.4



Fig. 2: Samples after compressive strength test

peak load. By using the following equation, the compressive strength can be calculated where  $P$  = Peak load,  $A$  = minimum cross-sectional area and  $F_c$  = compressive strength.

**The Thermal Conductivity, Diffusivity and Resistivity test:** The Linear heat source method is used to measure simultaneously the coefficients of conductivity and thermal diffusivity of the seven concrete samples. The storage capacity will be determined according to the relationship with conductivity and diffusivity.

In this test, a special thermal probe sensors needle coated with thermal grease (in order to maintain good contact with the concrete walls) is introduced into a drilled hole of 7 cm deep and 0.5 cm diameter in each of the seven concrete samples (samples A-D) and this is heated at constant power by the probe which also measures the temperature rise of the sample during the transient time through imbedded thermocouples. The probe sensors needle contains both a heating element and a thermistor. Its controller module contains a battery, a 16-bit micro-controller/AD converter and power control circuitry. The thermal properties analyzer (probe) is as shown in Fig. 3.



Fig. 3: Thermal properties analyzer

To start measurement with the probe, the microcontroller waits for 90 sec for temperature stability and then applies a known amount of current for 30 sec to a heater in the probe that has an accurately known resistance. The microprocessor calculates the amount of power supplied to the heater. The probe's thermistor measures the changing temperature for 30 sec while the microprocessor stores the data. At the end of the reading for each of the seven concrete samples the controller computes the thermal conductivity and diffusivity using the change in temperature  $\Delta T$  vs. time data. Thermal resistivity is computed as the reciprocal of thermal conductivity. It is important to wait for about 5 min between readings in order to make the probe to be as close to equilibrium as possible. An ideal environment for equilibrium can be accomplished by placing the probe in an isothermal chamber or styrofoam box.

## RESULTS AND DISCUSSION

The results of the observations and calculations are shown in Fig. 4-7. Tests were made on four concrete samples of cubic shape. Sample A consists of plain concrete without steel fibres; sample B consists of 5 cm length steel fibre plus concrete aggregates; sample C consists of 2.5 cm length steel fibre plus concrete fibre plus concrete aggregates.

The comparison of samples thermal conductivity were made with aggregates while sample D consists of 1 cm length steel temperatures and it was discovered that sample B which was reinforced with 5 cm steel fibres has the highest thermal conductivity while sample A of plain concrete has the lowest. The results indicate that there is very slight change of temperature for each of the concrete samples tested. The presence of steel fibres increases the thermal conductivity to a small extent. This increase in thermal conductivity can be attributed to the fact that the thermal conductivity of steel is about 50

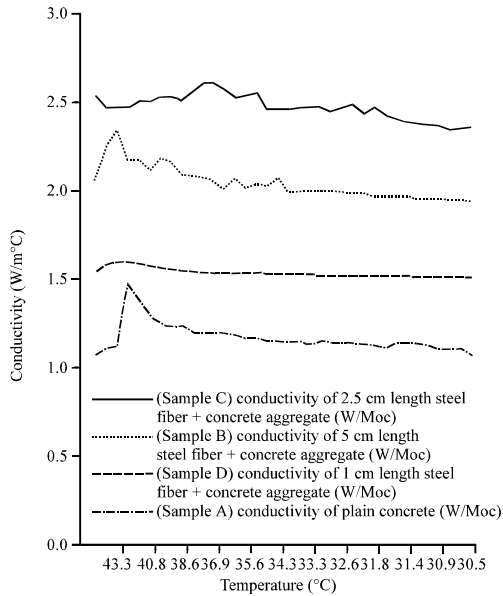


Fig. 4: Comparison of temperature with thermal conductivity of concrete samples A-D

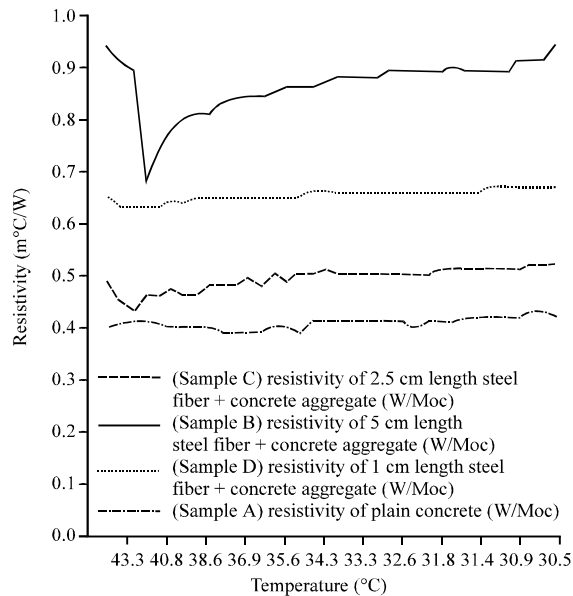


Fig. 5: Comparison of temperature with thermal resistivity of concrete samples A-D

times higher than that of concrete. The comparison of samples thermal conductivity were made with temperatures and it was discovered that sample B which was reinforced with 5 cm steel fibres has the highest thermal conductivity while sample A of plain concrete has the lowest. The results indicate that there is very slight change of temperature for each of the concrete samples tested. The presence of steel fibres increases the thermal conductivity to a small extent. This increase in

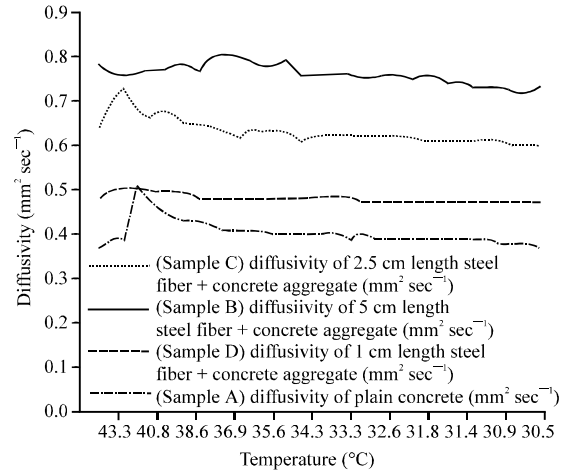


Fig. 6: Comparison of temperature with thermal diffusivity of concrete samples A-D

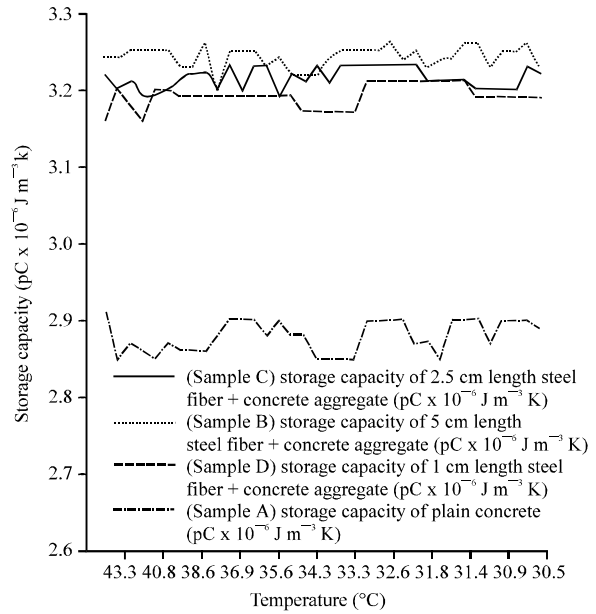


Fig. 7: Comparison of temperature with thermal storage capacity of concrete samples A-D

thermal conductivity can be attributed to the fact that the thermal conductivity of steel is about 50 times higher than that of concrete. From Fig. 5, it can be seen that thermal resistivity of the samples tested is an inverse of thermal conductivity. As shown in Fig. 6, sample B has the highest thermal diffusivity follow in order by samples C and D, respectively while sample A which consists of plain concrete has the lowest thermal diffusivity. This is an indication that the presence of steel fiber increases the rate at which a temperature disturbance at one point in the tested samples travels to another point. From the values shown in Table 3 for the densities of the samples tested,

sample B has the highest density follow in order by samples C and A, respectively while sample D has the lowest density. The increase in the density of the steel fibers reinforced concrete is due to the fact that steel has a density which is three times that of concrete and this actually improves the storage capacity of the samples with steel fibers as shown in Fig. 7.

The decrease in density noticed with sample D which contains 20 g steel fibers of length 1 cm may actually be due to the uniform dispersion of the fibers during the batching and mixing phase. It was noticed during calculation that the percentage of voids in samples D was about 25% while that of samples A-C range from 16-20%. It seems probable that the proportion of solid material to voids to a large extent determines the density, storage capacity and even the thermal conductivity. The storage capacity of sample A which is the lowest may be due to the fact that the sample contain only plain concrete without steel fibers.

The results of the measurements of the mechanical properties of the concretes samples showed that the compressive strength of the steel fiber reinforced concrete is higher than that of plain concrete as shown in Table 3. Compressive and tensile/flexural strengths are directly related to density. An increase in density of  $50-70 \text{ kg m}^{-3}$  can result in a compressive strength gain of  $5-8 \text{ N mm}^{-1}$  (12-18%). The compressive strength and density are slightly increased in value with steel fiber content with 0.66% as compared with the plain concrete with no steel fiber and the highest strength and density are obtained at the fiber-concrete ratio of 0.66% and 5 cm length steel fiber. The increase in compressive strength and bulk density may be due to the good homogeneity and high compaction between the steel fibers and the cement matrix.

However, the compressive strength of specimens increased with the increase in density, this can be explained by the fact that the composites have higher density and this might be due to the decrease in air void and low porosity. Steel fibers do little to enhance the static compressive strength of concrete with increases in strength ranging from essentially nil to perhaps 25%. Even in members which contain conventional reinforcement in addition to the steel fibers, the fibers have little effect on compressive strength.

However, the fibers do substantially increase the post-cracking ductility or energy absorption of the material. This is shown graphically in the compressive stress-strain curves of steel fiber reinforced concrete in Fig. 8. Fibers aligned in the direction of the tensile stress may bring about very large increases in direct tensile strength as high as 133% for 5% of smooth, straight steel

fibers. However for more or less randomly distributed fibers, the increase in strength is much smaller, ranging from as little as no increase in some instances to perhaps 60% with many investigations indicating intermediate values as shown in Fig. 9. Splitting-tension test of SFRC show similar result. Thus, adding fibers merely to increase the direct tensile strength is probably not worthwhile. However as in compression, steel fibers do lead to major

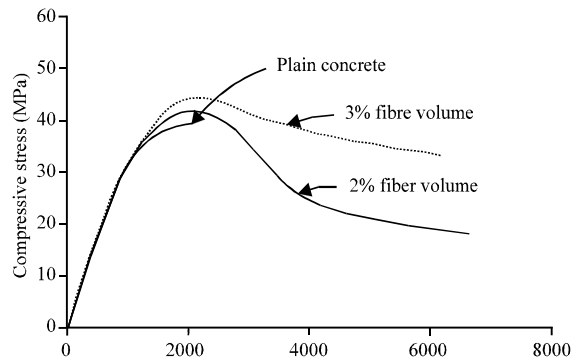


Fig. 8: Stress-strain curves in compression for steel fiber reinforced concrete (Johnston, 1974)

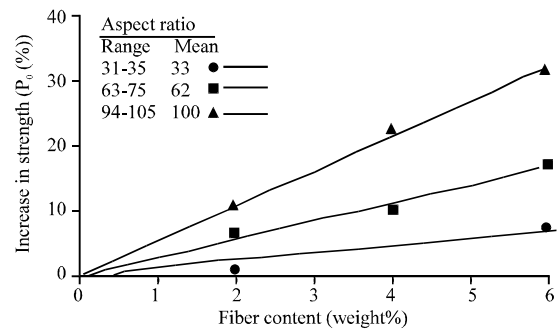


Fig. 9: Influence of steel fiber content on tensile strength (Johnston, 1974)

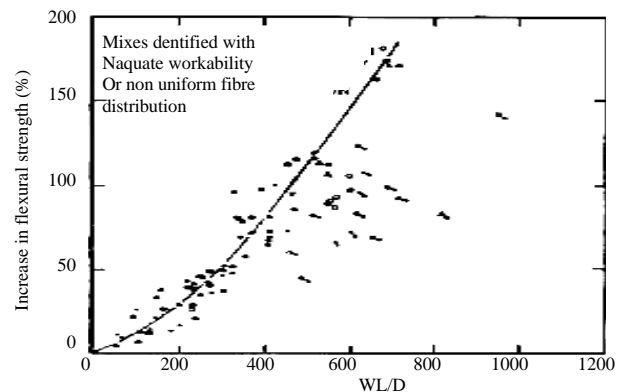


Fig. 10: Effect of WL/D on the flexural strength of concrete (Johnston, 1974)



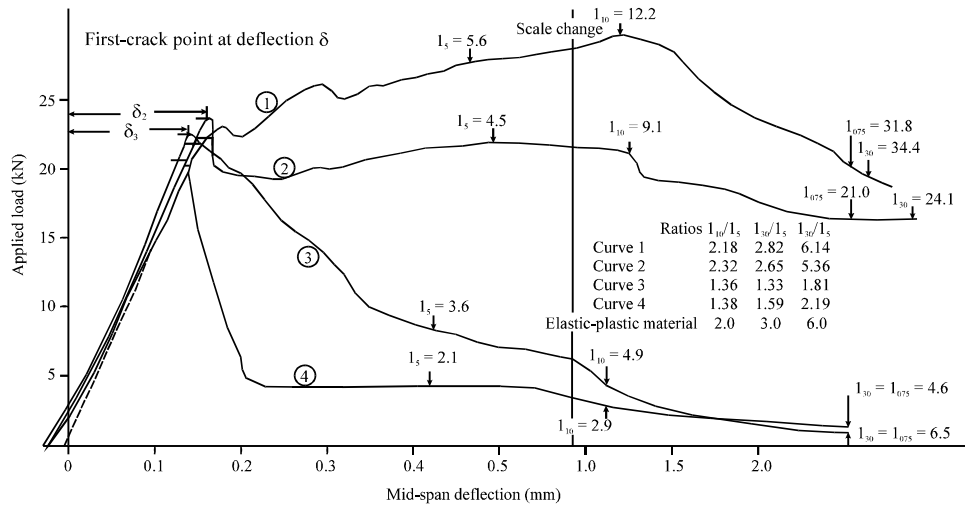


Fig. 11: Range of load-deflection curves obtained in the testing of steel fiber reinforced concrete (Johnston, 1982)

increases in the post-cracking behavior or toughness of the composites. Steel fibers are generally found to have aggregate much greater effect on the flexural strength of SFRC than on either the compressive or tensile strength with increases of >100% have been reported. The increase in flexural strength is particularly sensitive, not only to the fiber volume but also to the aspect ratio of the fibers with higher aspect ratio leading to larger strength increases. Figure 10 shows the fiber effect in terms of the combined parameter  $WL/D$  where  $L/D$  is the aspect ratio and  $W$  is the weight percent of fibers. It should be noted that for  $WL/D > 600$ , the mix characteristics tended to be quite unsatisfactory.

Deformed fibers show the same types of increases at lower volumes because of their improved bond characteristics. Fibers are added to concrete not to improve the strength but primarily to improve the toughness or energy absorption capacity.

Commonly, the flexural toughness is defined as the area under the complete load-deflection curve in flexure; this is sometimes referred to as the total energy to fracture. Alternatively, the toughness may be defined as the area under the load-deflection curve out to some particular deflection or out to the point at which the load has fallen back to some fixed percentage of the peak load.

Probably, the most commonly used measure of toughness is the toughness index proposed by Johnston and incorporated into ASTM C1018. As is the case with flexural strength, flexural toughness also increases at the parameter  $WL/D$  increases as show in Fig. 11.

The load-deflection curves for different types and volumes of steel fibers can vary enormously as was

shown previously in Fig. 11. For all of the empirical measures of toughness, fibers with better bond characteristics (i.e., deformed fibers or fibers with greater aspect ratio) give higher toughness values than do smooth, straight fibers at the same volume concentrations.

## CONCLUSION

Experimental studies were carried out to investigate the influence of steel fibers on the behaviour of concrete for the purpose of solar/thermal energy storage. It can be concluded that:

- The compressive strength of concrete reinforced with steel fiber is higher than that of plain concrete. The presence of steel fibers improves the ductility of a fiber reinforced concrete
- The presence of steel fibers also increases the thermal conductivity and thermal storage capacity of the concrete which makes it more suitable for energy storage

## REFERENCES

- ACI Committee, 1982. State-of-the art report in fiber reinforced concrete. ACI 554 IR-82, Detroit, MI., USA.
- ASTM C1018-89, 1991. Standard test method for flexural toughness and first crack strength of fibre reinforced concrete (Using beam with third-point loading). Book of ASTM Standards, Part 04.02, American Society for Testing and Materials, Philadelphia, USA., pp: 507-513.

- Adeyanju, A.A. and K. Manohar, 2009. Theoretical and experimental investigation of heat transfer in packed beds. *Res. J. Applied Sci.*, 4: 166-177.
- Adeyanju, A.A, T.O. Oni and D.O. Akindele, 2010. Experimental determination of thermo physical properties of concrete for thermal energy storage. *Int. J. Eng. Applied Sci.*, 5: 282-289.
- Balaguru, P.N. and S.P. Shah, 1992. *Fiber Reinforced Cement Composites*. McGraw Hill International, New York, USA., ISBN-13: 9780070564008, pp: 530.
- JCI, 1983. JCI standards for test methods of fiber reinforced concrete. *Method of Test for Flexural Strength and Flexural Toughness of Fiber Reinforced Concrete (Standard SF4)*, Japan Concrete Institute, Japan, pp: 45-51.
- Johnston, C.D., 1974. *Steel fiber reinforced mortar and concrete: A review of mechanical properties*. Fiber Reinforced Concrete ACI-SP 44, Detroit, USA.
- Johnston, C.D., 1982. Definition and measurement of flexural toughness parameters for fiber reinforced concrete. *Cem. Concr. Aggregate*, 4: 8-8.